J Nanopart Res (2017) 19: 131
DOI 10.1007/s11051-017-3803-0

RESEARCH PAPER

Synthesis and adsorption properties of hierarchical Fe_3O_4@MgAl-LDH magnetic microspheres

Xiaoge Wu · Bo Li · Xiaogang Wen

Received: 31 October 2016 / Accepted: 21 February 2017 / Published online: 30 March 2017

Abstract In this study, Fe_3O_4 microspheres were prepared by a hydrothermal method, and then the synthesized Fe_3O_4 microspheres were used as template to prepare Fe_3O_4@MgAl-LDH composite microspheres by a coprecipitation process. Morphology, composition, and crystal structure of synthesized nanomaterials were characterized by X-ray powder diffractometry, scanning electron microscopy, and Fourier transform infrared spectroscopy technologies. The composite hierarchical microspheres are composed of inner Fe_3O_4 core and outer MgAl-LDH-nanoflake layer, and the average thickness of MgAl-LDH-nanoflake is about 70 nm. The adsorption property of the products toward congo red was also measured using UV–vis spectrometer. The result demonstrated that the Fe_3O_4@MgAl-LDH composite adsorbent could remove 99.8% congo red in 30 min, and the maximum adsorption capacity is about 404.6 mg/g, while congo red removal rate of pure MgAl-LDH and Fe_3O_4 are only 86.3 and 53.1% in 40 min, respectively, and their adsorption capacity are 345.72 and 220.56 mg/g, respectively. It indicates the composite Fe_3O_4@ MgAl-LDH nanomaterials have better adsorption performance than pure Fe_3O_4 and MgAl-LDH nanomaterials. In addition, the magnetic nanocomposites could be separated easily, and it demonstrated good cycle performance.

X. Wu · B. Li · X. Wen (✉)
School of Materials Science and Engineering, Sichuan University, Chengdu 610065, People's Republic of China
e-mail: wenxg@scu.edu.cn

Keywords Fe_3O_4 · MgAl-LDH · Microsphere · Nanomaterials · Adsorption · Measurement method · Core-shell nanocomposites

Introduction

In recent years, organic dye pollutants produced by various dyestuff manufactures, plastic, paper, textile, cosmetics, leather, pharmaceutical, food, and other industries are frequently found in groundwater, and this is becoming a serious environmental and health problem. Obviously, the removal of color synthetic organic dye stuff from waste effluents becomes environmentally important. It is rather difficult to treat these dyes due to their complex molecular structure and xenobiotic properties. Many methods, including adsorption (Arami et al. 2006), ion-exchange (Liu et al. 2007), photocatalytic degradation (Muruganandham and Swaminathan 2006), chemical oxidation (Dutta et al. 2001), ozone treatment (Selcuk 2005), membrane filtration (Buonomenna et al. 2009), precipitation (Lee et al. 2006), flocculation (Lee et al. 2006), coagulation (Lee et al. 2006), and biological treatment (Kornaros and Lyberatos 2006) have been investigated to remove dyes from aqueous systems. Among these chemical, physical, or biological treatment processes, adsorption is the most promising one for the removal of dyes, mainly because of its high effectiveness and low cost and simplicity. Various kinds of materials including activated carbons (Degs et al. 2001), zeolite (Faki et al. 2008), fly-ashes (Janos et al. 2003), wood (Mckay and Poots 1980), pith (Namasivayam and Kanchana 1992),

clay (Ozcan and Ozcan 2004; Wang et al. 2004; Kacha et al. 1997), polymer (Ai et al. 2010; Kopinke et al. 2001), graphene (Sharma and Das 2013), porous metal–organic frameworks (Yang et al. 2011), and titanium peroxide (Zhao et al. 2014) could be used to adsorb dyes from waste water.

Layered double hydroxides (LDHs), well known as hydrotalcite-like compounds, can be expressed in general as $[M^{II}_{1-x}M^{III}_{x}(OH)_2]^{x+}A^{n-}_{x/n}\,m{\cdot}H_2O$, where, M^{II} and M^{III} are the divalent and trivalent cations, respectively. A^{n-} is the charge-balancing interlayer gallery anion (Meyn et al. 1990; Woo et al. 2011; Chang et al. 2005) and easy to exchange with other anions. Due to its excellent stability, unique microstructure and chemical composition, exchangeable interlayer anions, compositional flexibilities, large surface areas, ease of preparation, and low cost, LDHs have been widely used as adsorbents or exchangers to remove various anionic species in waste water. For example, LDHs and its derivatives with different composition and morphology have been used to remove anionic and cationic dyes (Aguiar et al. 2013), indigo carmine dyes (EI Gaini et al. 2009), acid green (dos Santos et al. 2013), methyl orange (Ai et al. 2011), orange II (Abdelkader et al. 2011), and anionic relative dye (Ahmed and Gasser 2012).

The LDHs commonly used to remove dyes from industrial effluent are the form of powder, it must be recovered by solid–liquid separation subsequent to the purification process. The separation and regeneration of adsorbent is one of the key to influence its application. If an adsorbent is magnetic, it can be readily separated from complex multiphase systems by applying an external magnetic field. Recently, Chen et al. reported the synthesis of the colloidal Fe_3O_4-LDH nanohybrids via an electrostatic interaction between the Fe_3O_4 nanoparticle and LDH nanoparticle, and it demonstrated excellent performance for removal of organic dyes in water (Chen et al. 2011), but the synthesis processes of Fe_3O_4 nanoparticles and LDH nanoparticles are tedious. Pan et al. have synthesized Fe_3O_4@DFUR-LDH submicro particles and exhibited its application in controlled drug delivery and release (Pan et al. 2011). In this paper, we synthesized core/shell Fe_3O_4@MgAl-LDH microspheres by a simple template-induced growth process, and the Fe_3O_4@MgAl-LDH microspheres demonstrated excellent adsorption performance toward congo red (CR); furthermore, it can be separated and regenerated easily. To our knowledge, this unique Fe_3O_4@MgAl-LDH microsphere with excellent adsorption ability has not been reported yet.

Experimental

Materials

Congo red used for this study was purchased from Tianjin Damao Reagent Factory. The chemicals, $FeCl_3{\cdot}6H_2O$, NaAc, ethylene glycol, ethanediamine, Na_2CO_3, NaOH, $Al(NO_3)_3{\cdot}9H_2O$, $Mg(NO_{3)2}{\cdot}6H_2O$, polyethylene glycol 20,000 (PEG-20000), and H_2O were all of analytical grade and obtained from Kelong Chemical Reagent Co. Ltd., (China). The desired pH was adjusted by adding NaOH and Na_2CO_3 (2:1).

Synthesis of Fe_3O_4 nanospheres

The Fe_3O_4 microspheres were synthesized by a hydrothermal process. At first, $FeCl_3.6H_2O$ (1.35 g) was dissolved in ethylene glycol (40 mL), followed by the addition of NaAc (3.6 g) providing the weak base environment and PEG-20000 (1 g) which will be an active agent. The mixture was vigorously mechanical stirred for 30 min. Then, the solution was transferred into a teflon-lined stainless steel autoclave (100 mL capacity) for hydrothermal treatment at 200 °C for 18 h. After cooling to room temperature, the black precipitate was collected by a magnet and washed several times using ethanol and water in sequence. Finally, the sample was dried overnight at 60 °C.

Synthesis of MgAl-LDH and Fe_3O_4@MgAl-LDH microspheres

The magnetic Fe_3O_4@MgAl-LDH microspheres were prepared by a coprecipitation method. The synthesized Fe_3O_4 microspheres (0.5 g) were ultrasonically dispersed into 50-mL water/methanol mixed solution (methanol/water = 1:1) in a 500-mL round bottom flask to obtain a uniform suspension; then, the flask was put into 60 °C oil bath under vigorous stirring. Four grams NaOH and 5.3 g Na_2CO_3 were dissolved in 1 L aqueous methanol as solution A; 1.155 g $Mg(NO_3)_2{\cdot}6H_2O$ and 0.565 g $Al(NO_3)_3{\cdot}9H_2O$ were dissolved in aqueous methanol as solution B. The A was added to B and kept the pH at about 10. The mixed A and B (1:1) solution was added to the round bottom drop by drop. After

being aged in solution for 24 h, the precipitate was washed with deionized water for several times; finally, the product was dried at 100 °C for 6 h.

Pure MgAl-LDH nanoflakes were synthesized by the same process in the absence of Fe_3O_4 microspheres.

Characterization methods

Morphology of Fe_3O_4, MgAl-LDH, and Fe_3O_4@MgAl-LDH composite were characterized using the scanning electron microscope (SEM, JEOLS-3400N, Japan). X-ray powder diffractometry (XRD) patterns of products were obtained from DX 1000 X-ray diffractometer (Philip, Netherland) with Cu Ka radiation (40 kV, 300 mA, λ = 0.154 nm) to confirm the structure of the material, the XRD data were collected in a scan range from 5 to 80°(2θ) with a step size of 0.03°. Nitrogen adsorption and desorption isotherm was measured using micromeritics tristar II3020 sorptometer. The specific surface area of the sample was derived using the multipoint Brunauer–Emmett–Teller (BET) method and the pore-size distribution was determined using the Barret–Joyner–Halenda (BJH) mathematical model. Fourier transform infrared spectroscopy (FTIR) spectra were recorded in the range of 4000–400 cm^{-1} on a FTIR spectrometer (Nicolet-6700, USA). UV–vis absorbance of products was measured by using UV1101 spectrophotometer (Techcomp).

Adsorption experiments

The adsorption performance of synthesized materials toward congo red was studied. Solutions containing the dye were prepared by dissolving a known quantity of the dye in DI water (1000 mg/L), followed by serial dilutions to reach the needed concentrations. All the adsorption experiments were conducted under stirring conditions throughout the test at room temperature (25 °C) in the dark. Twenty milligrams of as-prepared adsorbent was added to 50 mL of dye solutions (100 mg/L). At appropriate time intervals, the aliquots were withdrawn from the solution and the adsorbents were separated from the suspension via magnet. The concentration of residual CR in the supernatant solution was detected using a UV–vis spectrophotometer at the 500 nm. The sampling continued until the adsorption process reaches its equilibrium. Every adsorption experiment was repeated three times.

The removal efficiency of dye was given according to the following formula:

$$\text{removal}\,(\%) = \frac{(C_0 - C_t)}{C_0} \times 100\%$$

where C_0 (mg/L) is the initial concentration of adsorbent, C_t (mg/L) is the concentration of adsorbate at time t (min).

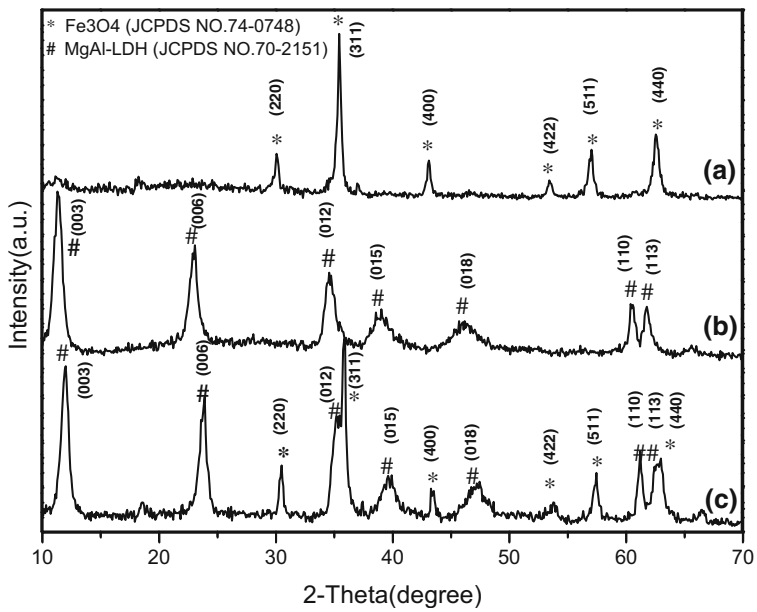

Fig. 1 XRD patterns of *(a)* pure Fe_3O_4, *(b)* pure MgAl-LDH, and *(c)* composite Fe_3O_4@MgAl-LDH nanomaterials

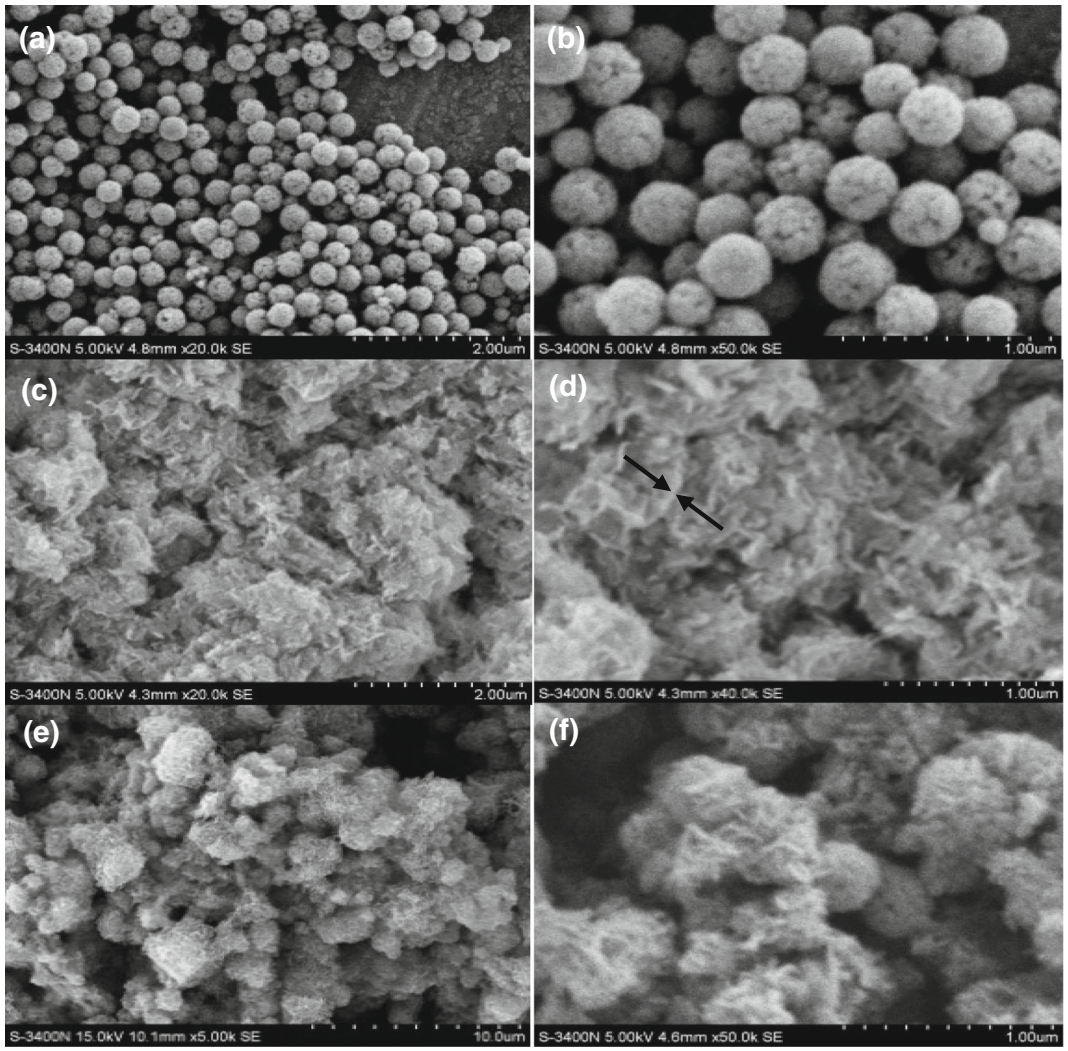

Fig. 2 SEM images with different magnification of pure Fe_3O_4 (**a**, **b**), pure MgAl-LDH (**c**, **d**), and composite Fe_3O_4@MgAl-LDH (**e**, **f**) nanomaterials

The adsorption capacity q_e (mg/g) was calculated by the following formula:

$$qe = \frac{(C_0 - C_e)V}{m}$$

where C_e (mg/L) is the concentration of the adsorbate at equilibrium, V (L) is the volume of adsorbate solution, and m (g) is the mass of adsorbent.

The recycling of the adsorbent was evaluated by repeating cycles of adsorption–separation–regeneration using the same Fe_3O_4@MgAl-LDH sample. After the adsorption, the adsorbent was separated by a magnet, then it was annealed in a tube furnace at 400 °C for 6 h. Appropriate new adsorbent was added into recycled sample to replenish the adsorbent lost (about 5%) in the adsorption, separation, regeneration process.

Results and discussion

Figure 1 shows the XRD patterns of pure and composite materials. The diffraction patterns shown by curve (a) and curve (b) can be well indexed to a cubic phase of Fe_3O_4 (JCPDS NO.74-0748) and MgAl-LDH (JCPDS NO.70-2151), respectively. The XRD pattern shown in Fig. 1c clearly indicates that the final product is a mixture of Fe_3O_4 and MgAl-LDH; all the diffraction peaks can be attributed to cubic Fe_3O_4 and MgAl-LDH. The peaks at

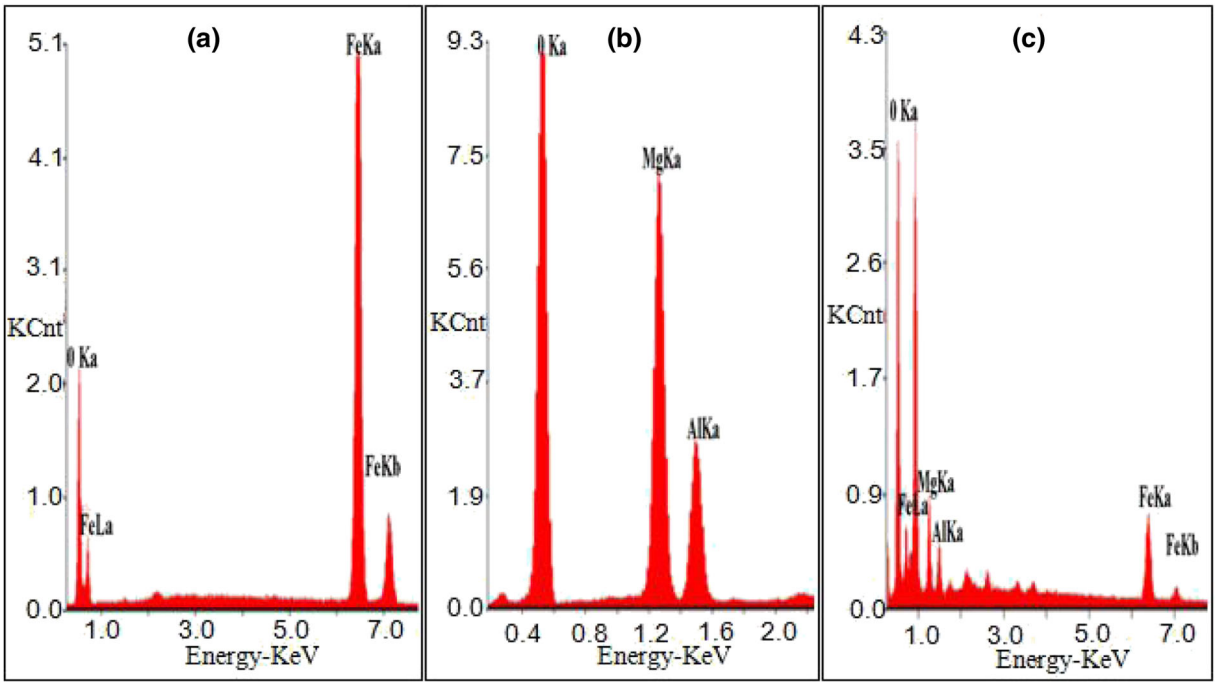

Fig. 3 EDS spectra of Fe_3O_4 microspheres (**a**), MgAl-LDH nanoflakes (**b**), and Fe_3O_4@MgAl-LDH core/shell microspheres (**c**)

30.1°, 35.4°, 43.1°, 53.4°, 56.9°, and 62.5° come from the (220), (311), (400), (422), (511), and (440) of Fe_3O_4, and the signal at 11.6°, 23.3°, 34.9°, 38.1°, 44.4°, and 60.7° come from the (003), (006), (012), (015), (018), (110), and (113) of MgAl-LDH, and there is no other impurity.

The SEM images of Fe_3O_4, MgAl-LDH, and Fe_3O_4@MgAl-LDH are shown in Fig. 2. The pure Fe_3O_4 is sphere-like structure with an average diameter (the average diameter of all the particles in a SEM field of view was calculated) of 350 nm; many nanopores can be observed on the surface of Fe_3O_4 microspheres (Fig. 2a). Based on SEM image with higher magnification, it demonstrates that Fe_3O_4 porous microspheres are comprised of many smaller nanoparticles with a diameter about 20 nm (Fig. 2b). The pure MgAl-LDH is flake-like nanostructures with an average thickness of about 70 nm (labeled with black arrows in Fig. 2d. Figure 2e, f shows the SEM images of hybrid Fe_3O_4@MgAl-LDH product; it indicates that the hybrid nanostructures are hierarchical microspheres, which consist of inner Fe_3O_4 core and outer MgAl-LDH nanoflake shell. The average diameter of the Fe_3O_4@MgAl-LDH microspheres is about 430 nm, which is a little larger than that of pure Fe_3O_4 microspheres, and the size of inner Fe_3O_4 core has no obvious change; it suggests that the Fe_3O_4 microspheres act as a template to induce the deposition and growth of MgAl-LDH; finally, core/shell Fe_3O_4@MgAl-LDH microspheres are obtained.

Figure 3 shows the energy dispersive spectroscopy (EDS) spectra of Fe_3O_4 microspheres, MgAl-LDH nanoflakes, and Fe_3O_4@MgAl-LDH core/shell microspheres, and Table 1 lists the corresponding element analysis result. As we can see, the measured Fe:O molar ratio of pure Fe_3O_4 microspheres is about 0.78, which is agreement with the atom ratio in the Fe_3O_4. The measured Mg:Al molar ratio in pure MgAl-LDH and

Table 1 Element analysis of Fe_3O_4 microspheres, MgAl-LDH nanoflakes, and Fe_3O_4@MgAl-LDH core/shell microspheres

Sample	%Mg (At%)	%Al (At%)	%Fe (At%)	%O (At%)	Mg:Al	Fe:O
Fe_3O_4	–	–	40.47	51.53	–	0.78
MgAl-LDH	23.15	10.19	–	65.97	2.2	–
Fe_3O_4@MgAl-LDH	11.5	5.12	13.38	70.0	2.3	–

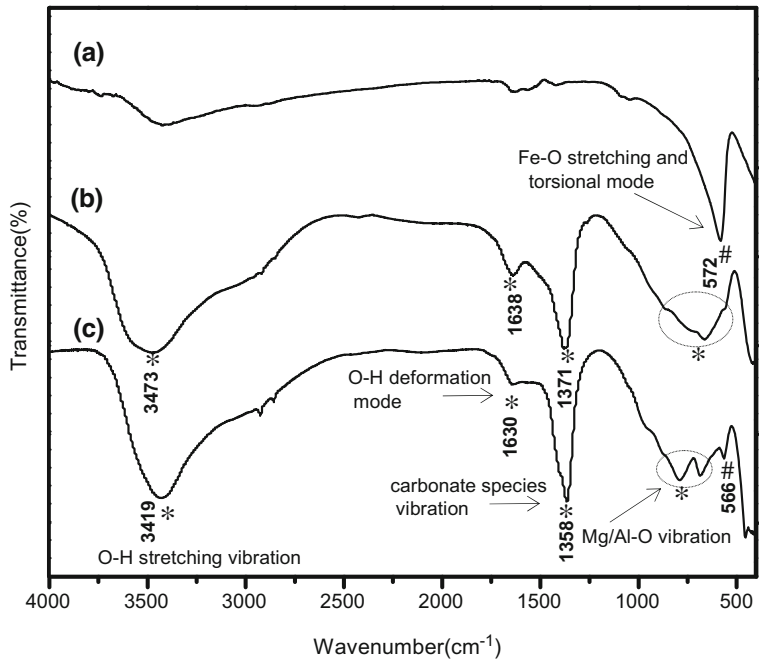

Fig. 4 FTIR spectra of Fe_3O_4 (**a**), MgAl-LDH (**b**), and Fe_3O_4@MgAl-LDH (**c**)

composite Fe_3O_4@MgAl-LDH are about 2.2 and 2.3, respectively, which are smaller than the value in the precursor solution (3.0). A similar observation was reported earlier due to the leaching of Mg^{2+} under the current synthesis conditions (Ai et al. 2011; EI Gaini et al. 2009; Abdelkader et al. 2011).

The FTIR spectra of the pure Fe_3O_4, pure MgAl-LDH, and composite Fe_3O_4@MgAl-LDH are shown in Fig. 4. In curve (a), the absorption band observed around 572 cm^{-1} belongs to Fe-O stretching and torsional mode of Fe_3O_4 (Racuciu 2009). In curve (b), the strong and broad absorption band observed around 3473 cm^{-1} corresponds to the O-H stretching vibration of the layer surface and/or interlayer water molecules (Ai et al. 2011; EI Gaini et al. 2009; Abdelkader et al. 2011). The adsorption peaks in the range of 500–

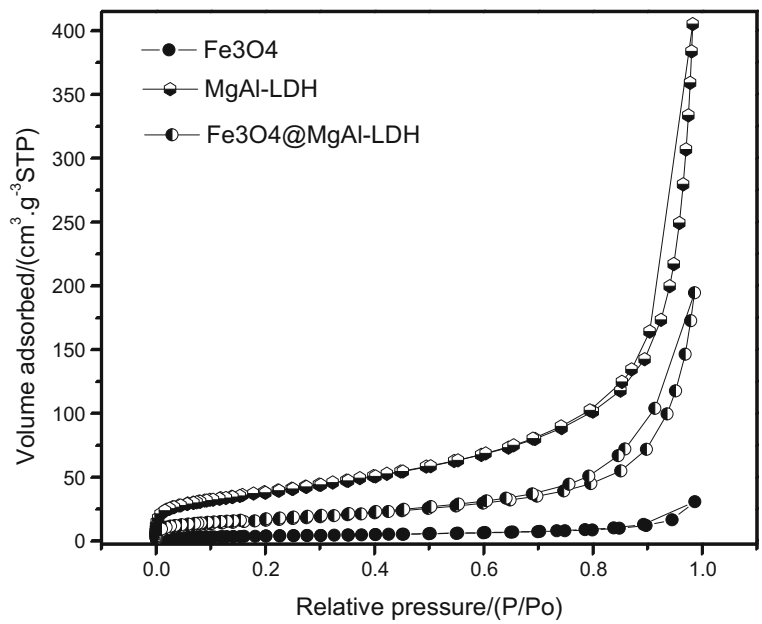

Fig. 5 N_2 adsorption–desorption isotherms (at −196 °C) of Fe_3O_4, MgAl-LDH, and Fe_3O_4@MgAl-LDH nanomaterials

800 cm^{-1} are associated with M-O, O-M-O, and M-O-M lattice vibrations (M = Mg and Al) (Ai et al. 2011; EI Gaini et al. 2009; Abdelkader et al. 2011). The strong peak at 1371 cm^{-1} is due to the interlayer carbonate species (mode v3) in the MgAl-LDH (Ai et al. 2011; Abdelkader et al. 2011), and the band at 1636 cm^{-1} belongs to the hydroxyl deformation mode of the water molecules in the interlayer (Ai et al. 2011; Abdelkader et al. 2011). The FTIR spectrum of composite Fe_3O_4@MgAl-LDH mainly demonstrates the MgAl-LDH absorption (3419, 1630, 1358, 762 cm^{-1}) companying a weaker Fe_3O_4 adsorption at around 570 cm^{-1}(curve (c)); the weaker absorption of Fe_3O_4 can be attributed to the coating of LDH on the surface of Fe_3O_4. The strong peak at 1358.74 cm^{-1} comes from the interlayer carbonate species, which act as charge-balancing interlayer anion in MgAl-LDH.

The specific surface area and porosity of the as-prepared samples were determined by nitrogen adsorption measurements. Figure 4 displays the N_2 adsorption–desorption isotherms and the corresponding pore-size distribution curve for pure Fe_3O_4, pure MgAl-LDH, and composite Fe_3O_4@MgAl-LDH microspheres. All the pure Fe_3O_4, MgAl-LDH, and composite Fe_3O_4@MgAl-LDH microspheres exhibit a typical IV isotherm with a narrow hysteresis loop according to IUPAC classification (Rouquerol et al. 1994). The measured specific surface area of Fe_3O_4, MgAl-LDH, and Fe_3O_4@MgAl-LDH microspheres is 13.46, 139.47, and 57.2 m^2/g, respectively. Although the aggregation of magnetic Fe_3O_4 and Fe_3O_4@MgAl-LDH nanostructures induced smaller specific surface area than pure MgAl-LDH, the specific surface area of

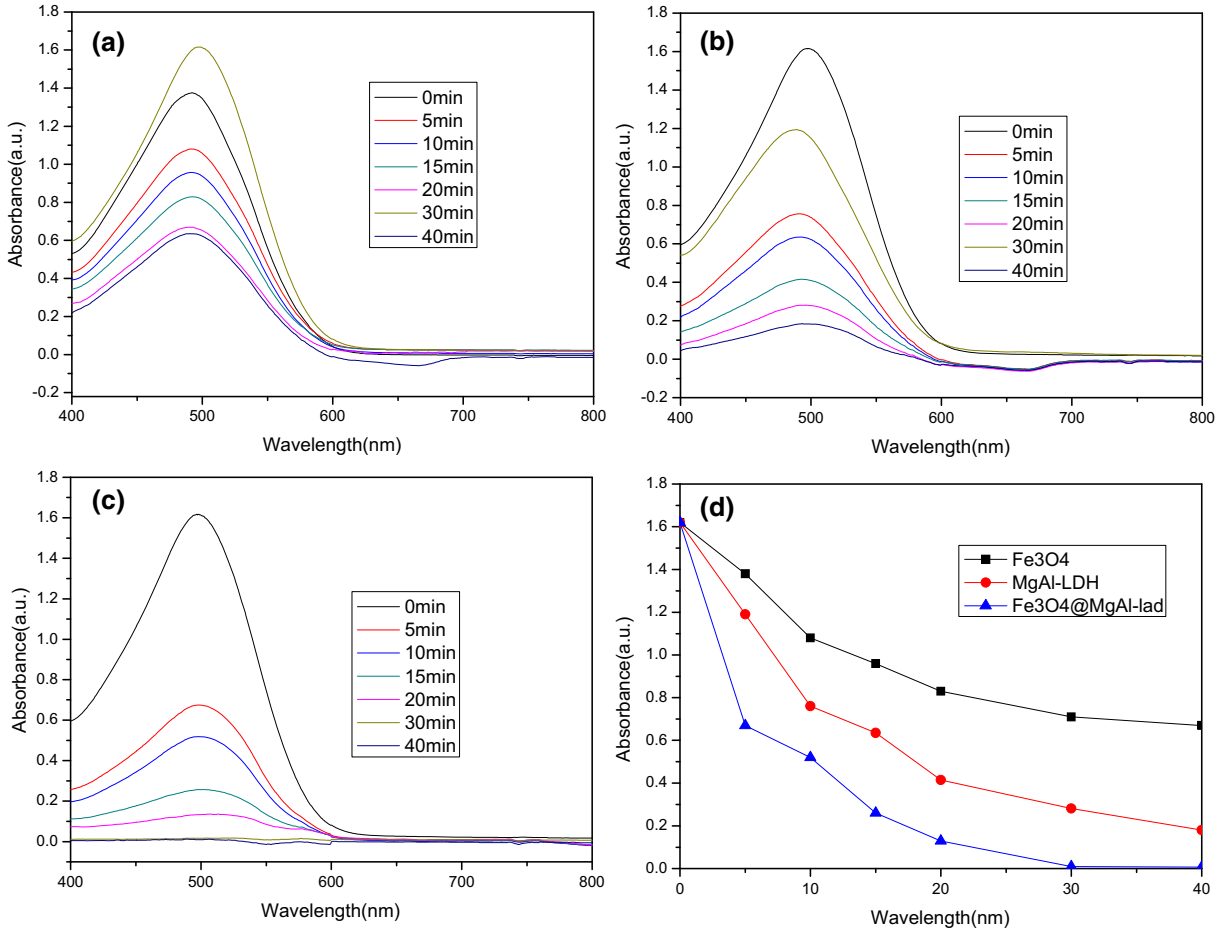

Fig. 6 the UV–vis spectra of congo red solutions after different contact time in the presence of pure Fe_3O_4 microspheres (**a**), pure MgAl-LDH nanoflakes (**b**), and Fe_3O_4@MgAl-LDH nanocomposite (**c**); and the removal efficiency of different adsorbent toward CR (**d**). (Initial concentration 100 mg/L, catalyst dosage 0.2 g/L, temperature 25 °C)

Fe_3O_4@MgAl-LDH increase about four times than that of pure Fe_3O_4 microspheres.

The adsorption performance of synthesized nanomaterials was studied. Figure 6 shows the UV–vis spectra of congo red solutions after different contact time in the presence of different adsorbent. The pure Fe_3O_4 microspheres have weak adsorption ability toward CR; it is able to slowly (within 40 min) adsorb 53.1% of congo red with an initial concentration of 100 mg/L; the adsorption capacity is about 220.56 mg/g (Fig. 6a, d). The adsorption capacity of Fe_3O_4 microspheres should come from its porous microstructures, but its small surface area lead to its lower adsorption performance. The MgAl-LDH nanoflakes show a much better adsorption ability than pure Fe_3O_4 microspheres; it can adsorb 86.3% of CR in 40 min; the adsorption capacity is about 345.72 mg/g (Fig. 6b, d). The MgAl-LDH nanoflakes have a larger specific surface and a plate-like structure, and the anionic CR can exchange with CO_3^{2-} anions of MgAl-LDH (Shan et al. 2014), at the same time, due to the memory effect, the intercalation induced by microstructure reconstruction of LDHs will also improve the adsorption (Crepaldi et al. 2002), so it demonstrates good adsorption ability. Although the composite Fe_3O_4@MgAl-LDH microspheres have a smaller specific surface area than pure MgAl-LDH nanoflakes (Fig. 5), it demonstrates better adsorption ability than both pure Fe_3O_4 microspheres and pure MgAl-LDH nanoflakes (Fig. 6c, d). Of the CR, 99.8% can be removed by Fe_3O_4@MgAl-LDH microspheres in 30 min; its adsorption capacity can reach to 404.6 mg/g. The excellent adsorption performance can be attributed to its unique microstucture. The growth of MgAl-LDH nanoflakes on the surface of Fe_3O_4 microspheres improves the dispersity of MgAl-LDH nanoflakes which mainly provide adsorption site in the nanocomposites, and the hierarchical microstructures filled with micropores and tunnels which facilitate the reserve of adsorbed dye molecular. LDHs can uptake anions from a solution by three different machanisms: adsorption, intercalation by anion exchange, and intercalation by reconstruction of calcined precursor (Crepaldi et al. 2002). Due to the carbonate, which presents strong electrostatic interaction with the layers, is difficult to exchange, in this composite Fe_3O_4@MgAl-LDH microsphere system, dye anions are mainly uptaken by adsorption and intercalation induced by reconstruction of calcined LDHs. Due to the presence of magnetic Fe_3O_4 cores, the composite Fe_3O_4@MgAl-LDH adsorbent can

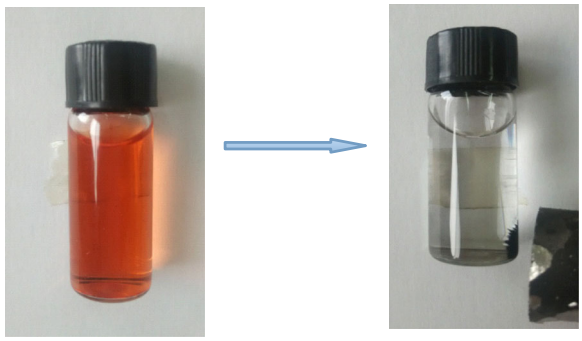

Fig. 7 Micrographs of dye solution before and after adsorption and separation

be quickly separated by a magnet. Figure 7 shows the micrographs of dye solution before and after adsorption and separation. It is clear that the red CR solution become colorless after Fe_3O_4@MgAl-LDH treatment for 40 min, and the black adsorbent can be easily separated from the solution by a magnet.

The regeneration ability is an important consideration for the application of adsorbent. The commonly reported regeneration methods include chemical oxidation, solvent, and thermal regeneration (Boulinguiez and Cloirec 2010; Song et al. 2009; Wang et al. 2006; Tamon and Okazak 1997; Huling et al. 2007, 2005). Here, we applied thermal technology for regeneration of our used nanocomposite adsorbent due to the high efficiency and low cost of thermal treatment process. After heat treatment at 400 °C for 6 h, the dye could be removed from adsorbent, and the structure of adsorbent

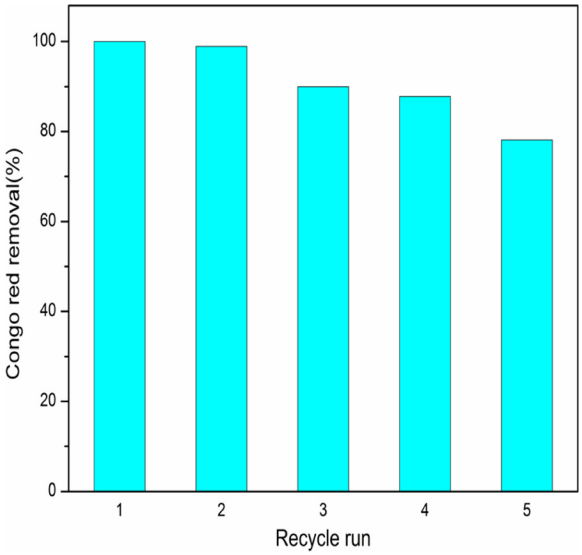

Fig. 8 CR remove rate of Fe_3O_4@MgAl-LDH after different recycle runs

could restore to the original state before adsorption. Figure 8 shows the CR remove rate of Fe_3O_4@MgAl-LDH after different recycle runs. The CR remove rate can reach to 99.3% at the second run, and it can retain to about 78.1% after 5 cycle runs. The decrease of adsorption ability can be attributed to the partial destruction of MgAl-LDH microstructure and the remanent impurity comes from dye which take up the adsorption site after repeated adsorption and heat treatment.

Conclusions

A novel hierarchical Fe_3O_4@MgAl-LDH composite nanomaterial with good adsorption performance has been successfully synthesized. The composite microspheres composed of inner Fe_3O_4 core and outer MgAl-LDH-nanoflake layer. Under a magnetic field, it could be easily separated from the solution. The Fe_3O_4@MgAl-LDH composite microspheres exhibit excellent adsorption performance toward congo red in the solution. It demonstrates a high adsorption capacity of 404.6 mg/g, and the saturated adsorption capacity of pure Fe_3O_4 and MgAl-LDH is only 220.56 and 345.72 mg/g, respectively. Furthermore, the composite microspheres exhibit fast adsorption rate; 99.8% CR could be removed in 30 min, which is much higher than that of pure Fe_3O_4 (53.1%) and MgAl-LDH (86.3%). The used nanocomposite adsorbent can be fast separated by the magnet and regenerated using thermal treatment. It was found that about 78.1% of CR removal rate can still be retained after five recycle runs. The Fe_3O_4@MgAl-LDH nanocomposites combined nanostructured and magnetic features should be a potential adsorbent with excellent performance.

Acknowledgements This work was supported by the Scientific Research Foundation for the Returned Overseas Chinese Scholars, State Education Ministry, the National Natural Science Foundation of China (Grant Nos. 50872084 and 51072124), Program for New Century Excellent Talents in University (No. NCET100605). We wish to thank the Analytical & Testing Center of Sichuan University (SCU) for the assistance in sample characterization.

Compliance with ethical standards

Funding This study was funded by the Scientific Research Foundation for the Returned Overseas Chinese Scholars, State Education Ministry, the National Natural Science Foundation of China (Grant Nos. 50872084 and 51072124), Program for New Century Excellent Talents in University (No. NCET100605).

Conflict of interest The authors declare that they have no conflict of interest.

References

Abdelkader NBH, Bentouami A, Derriche Z, Bettahar N, DeMenorval LC (2011) Synthesis and characterization of Mg-Fe layer double hydroxides and its application on adsorption of Orange G from aqueous solution. Chem Eng J 169:231–238

Ahmed IM, Gasser MS(2012) Adsorption study of anionic reactive dye from aqueous solution to Mg–Fe-CO3 layered double hydroxide (LDH). Appl Surf Sci 259:650–656

Ai LH, Jiang J, Zhang R (2010) Uniform polyaniline microspheres: a novel adsorbent for dye removal from aqueous solution. Synth Met 160:762–767

Ai LH, Zhang CY, Meng LY (2011) Adsorption of methyl orange from aqueous solution on hydrothermal synthesized Mg–Al layered double hydroxide. J Chem Eng Data 56:4217–4225

Aguiar JE, Bezerra BTC, Braga BD, Lima PDD, Nogueira REFQ, Lucena SMP, Silva IJ (2013) Adsorption of anionic and cationic dyes from aqueous solution on non-calcined Mg-Al layered double hydroxide: experimental and theoretical study. Sep Sci Technol 48:2307–2316

Arami M, Limaee NY, Mahmoodi NM, Tbrizi NS (2006) Equilibrium and kinetics studies for the adsorption of direct and acid dyes from aqueous solution by soy meal hull. J Hazard Mater B135:171–179

Boulinguiez B, Cloirec PL (2010) Chemical transformation of sulfur compound adsorbed onto activated carbon materials during thermal desorption. Carbon 48:1558–1569

Buonomenna MG, Gordano A, Golemme G, Drioli E (2009) Preparation characterization and use of PEEKWC nano ltration membranes for removal of Azur B dye from aqueous media. React Funct Polym 69:259–263

Chang Z, Evans DG, Duan X, Vial C, Ghanbaja J, Prevot V, de Roy M, Foran C (2005) Synthesis of [Zn-Al-CO3] layered double hydroxides by a coprecipitation method under steady-state conditions. J Solid State Chem 178: 2766–2777

Chen CP, Gunawan P, Xu R (2011) Self-assembled Fe3O4-layered double hydroxide colloidal nanohybrids with excellent performance for treatment of organic dyes in water. J Mater Chem 21:1218–1225

Crepaldi EL, Tronto J, Cardoso LP, Valim JB (2002) Sorption of terephthalate anions by calcined and uncalcined hydrotalcite-like compounds. Colloids Surf A Physicochem Eng Asp 211: 103–114

dos Santos RMM, Gonçalves RGL, Constantino VRL, da Costa LM, da Silva LHM, Tronto J, Pinto FG (2013) Removal of Acid Green 68:1 from aqueous solutions by calcined and uncalcined layered double hydroxides. Appl Clay Sci 80-81:189–195

Degs YA, Khraisheh MAM, Allen SJ, Ahmad MNA (2001) Sorption behavior of cationic and anionic dyes from aqueous solution on different types of activated carbons. Sep Sci Technol 36:91–102

Dutta K, Mukhopadhyaya S, Bhattacharjee S, Chaudhuri B (2001) Chemical oxidation of methylene blue using a Fenton-like reaction. J Hazard Mater 84:57–71

EIGaini L, Lakraimi M, Sebbar E, Meghea A, Bakasse M (2009) Removal of indigo carmine dye from water to Mg-Al-CO3 calcined layered double hydroxides. J Hazard Mater 161: 627–632

Faki A, Turan M, Ozdemir O, Turan AZ (2008) Analysis of xedbed lumnadsorption of reactive yellow 176 onto surfactant-modi edzeolite. Ind Eng Chem Res 47:6999–7004

Huling SG, Jones PK, Ela WP, Arnold RG (2005) Fenton-driven chemical regeneration of MTBE-spent GAC. Water Res 39: 2145–2153

Huling SG, Jones PK, Lee TR (2007) Iron optimization for Fenton-driven oxidation of MTBE-spent granular activated carbon. Environ Sci Technol 41:4090–4096

Janos P, Buchtova H, Ryznarova M (2003) Sorption of dyes from aqueous solutions onto fly ash. Water Res 37:4938–4944

Kopinke FD, Georgi A, Mackenzie K (2001) Sorption of pyrene to dissolved humic substances and related model polymers.1. Structure–property correlation. Environ Sci Technol 35: 2536–2542

Kacha S, Ouali MS, Elmaleh S (1997) Dye abatement of textile industry wastewater with bentonite and alumininium salts. Rev Sci Eau 2:233–248

Kornaros M, Lyberatos G (2006) Biological treatment of wastewaters from a dye manufacturing company using a trickling filter. J Hazard Mater 136:95–102

Lee JW, Choi SP, Thiruvenkatachari R, Shim WG, Moon H (2006) Submerged microfiltration membrane coupled with alum coagulation/powdered activated carbon adsorption for complete decolorization of reactive dyes. Water Res 40:435–444

Liu CH, Wu JS, Chiu HC, Suen SY, Chu KH (2007) Removal of anionic reactive dyes from water using anion exchange membranes as adsorbers. Water Res 41:1491–1500

Mckay G, Poots VJP (1980) Kinetics and diffusion processes in colour removal from effluent using wood as an adsorbent. J Chem Technol Biotechnol 30:279–292

Meyn M, Beneke K, Lagaly G (1990) Anion-exchange reactions of layered double hydroxides. Inorg Chem 29:5201

Muruganandham M, Swaminathan M (2006) TiO2 UV photocatalytic oxidation of reactive yellow 14: eect of operational parameters. J Hazard Mater 135:78–86

Namasivayam C, Kanchana N (1992) Waste banana pith as adsorbent for color removal from wastewaters. Chemosphere 25: 1691-1705

Ozcan AS, Ozcan A (2004) Adsorption of acid dyes from aqueous solutions onto acid-activated bentonite. J Colloid Interf Sci 276:39–46

Pan DK, Zhang H, Fan T, Chen JG, Duan X (2011) Nearly monodispersed core-shell structural Fe3O4@DFUR-LDH submicro particles for magnetically controlled drug delivery and release. Chem Commun 47: 908–910

Racuciu M (2009) Synthesis protocol influence on aqueous magnetic fluid properties. Curr Appl Phys 9:1062–1066

Rouquerol J, Avnir D, Fairbridge CW, Everett DH, Haynes JH, Pernicone N, Ramsay JDF, Sing KSW, Unger KK (1994) Recommendations for the characterization of porous solids. Pure Appl Chem 66(8):1739–1758

Selcuk H (2005) Decolorization and detoxification of textile wastewater by ozonation and coagulation processes. Dyes Pigments 64:217–222

Shan RR, Yan LG, Yang K, Yu SJ, Hao YF, Yu HQ, Du B (2014) Magnetic Fe_3O_4/ MgAl-LDH composite for effective removal of three red dyes from aqueous solution. Chem Eng J 252: 38–46

Song Z, Chen LF, Hu JC, Richards R (2009) NiO(111) nanosheets as efficient and recyclable adsorbents for dye pollutant removal from waste water. Nanotechnology 20:275707

Sharma P, Das MR (2013) Removal of a cationic dye from aqueous solution using graphene oxide nanosheets: investigation of adsorption parameters. J Chem Eng Data 58:151 −158

Tamon H, Okazak M (1997) Influence of surface oxides on ethanol regeneration of spent carbonaceous adsorbents. J Colloid Interface Sci 196:120–122

Wang CC, Juang LC, Hsu TC, Lee CK, Lee JF, Huang FC (2004) Adsorption of basic dyes onto montmorillonite. J Colloid Interf Sci 273:80–86

Wang SB, Li HT, Xie SJ, Liu SL, Xu LY (2006) "Physical and chemical regeneration of zeolitic adsorbents for dye removal in wastewater. Chemosphere 65:82–87

Woo MA, Kim TW, Paek MJ, Ha HW, Choy JH, Hwang SJ (2011) Phosphate intercalated Ca-Fe-layered double hydroxides: crystal structure, bonding character, and release kinetic of phosphate. J Solid State Chem 184:171–176

Yang C, Kaipa U, Mather QZ, Wang XP , Nesterov V, Venero AF, Omary MA (2011) Fluorous metal-organic frameworks with superior adsorption and hydrophobic properties toward oil spill cleanup and hydrocarbon storage. J Am Chem Soc 133: 18094–18097

Zhao XG, Huang JG, Wang B, Bi Q, Dong LL, Liu XJ (2014) Preparation of titanium peroxide and its selective adsorption property on cationic dyes. Appl Surf Sci 292:576–582